



Article

Physiological Studies and Transcriptomic Analysis Reveal the Mechanism of Saline-Alkali Stress Resistance of *Malus sieversii* f. *niedzwetzkyana*

Lepu Jiang ¹, Yan Yang ¹, Zhengli Zhou ^{1,*} and Xuesen Chen ^{2,*}

¹ Key Laboratory of Biological Resources Protection and Utilization Corps of Tarim Basin, Tarim University, Alar 843300, China; jianglepu@163.com (L.J.); 10757213063@stumail.taru.edu.cn (Y.Y.)

² College of Horticulture Sciences, Shandong Agricultural University, No. 61 Daizong Road, Tai'an 271018, China

* Correspondence: zzzlkytd@163.com (Z.Z.); chenxs@sdau.edu.cn (X.C.)

Abstract: *Malus sieversii* f. *niedzwetzkyana*, a wild species capable of growing on saline-alkali soil in Xinjiang, is the most promising horticultural crop for improving the saline-alkali wasteland. However, the tolerance of *M. niedzwetzkyana* to saline-alkali stress and the underlying molecular mechanisms remains largely unknown. Here, we conducted a hydroponic experiment in which *M. niedzwetzkyana* and *M. domestica* “Royal Gala” seedlings were subjected to 150 mM saline-alkali stress. Physiological data showed that *M. niedzwetzkyana* had a strong ROS scavenging ability and ion transport ability, and its saline-alkali resistance was higher than that of *M. “Royal Gala”*. Saline-alkali stress also promoted the synthesis of anthocyanins in *M. niedzwetzkyana*. Transcriptome analysis was conducted on the leaves and roots of *M. niedzwetzkyana* at different time points under saline-alkali stress (0 h, 6 h, and 12 h). Transcriptome analysis revealed that saline stress down-regulated most genes involved in the anthocyanin flavonoid synthesis pathway. Transcription levels of genes involved in antioxidant enzyme activity and ion transport were altered. We identified hub genes related to superoxide dismutase as well as Na⁺ and K⁺ transport using weighted gene co-expression network analysis. This study elucidated, for the first time at the molecular level, the saline-alkali tolerance of *M. niedzwetzkyana*, including the complex changes in pathways that regulate reactive oxygen species homeostasis, ion uptake, and anthocyanoside synthesis under saline-alkali stress conditions. This research provides an important genetic resource for identifying genes involved in responses to saline-alkali stress.

Keywords: *Malus sieversii* f. *niedzwetzkyana*; saline-alkali stress; RNA-Seq; transcriptome analysis; candidate genes



Citation: Jiang, L.; Yang, Y.; Zhou, Z.; Chen, X. Physiological Studies and Transcriptomic Analysis Reveal the Mechanism of Saline-Alkali Stress Resistance of *Malus sieversii* f. *niedzwetzkyana*. *Horticulturae* **2024**, *10*, 510. <https://doi.org/10.3390/horticulturae10050510>

Academic Editors: Sara González-Orenga, M. Iftikhar Hussain and Muhammad Ikram

Received: 27 March 2024

Revised: 8 May 2024

Accepted: 11 May 2024

Published: 15 May 2024



Copyright: © 2024 by the authors. Licensee MDPI, Basel, Switzerland. This article is an open access article distributed under the terms and conditions of the Creative Commons Attribution (CC BY) license (<https://creativecommons.org/licenses/by/4.0/>).

1. Introduction

Soil salinization is a globally significant problem, and secondary salinization (i.e., salinization associated with human activities) is becoming increasingly common [1]. Salinization and alkalization affect approximately 20% of arable land and 33% of irrigated agricultural land globally due to inappropriate agricultural practices. Approximately 50% of the world's arable land is expected to be affected by salinization and alkalization by 2050 [2,3]. The apple (*Malus*) is one of the world's most economically important fruits, but its lack of saline-alkali tolerance has greatly limited the growth and yield of apple trees. *Malus sieversii* and its red-fleshed variant (*M. sieversii* f. *niedzwetzkyana*) are native to the mountains of Xinjiang and Central Asia; they are important wild apple resources and are considered the most primitive species [4,5]. *M. sieversii* is a wild species that can grow on saline soil in Xinjiang; it also has a high tolerance to drought and other types of stress, and these properties make it a valuable germplasm for the breeding of apple varieties with

saline-alkali tolerance. Studies aimed at clarifying the underlying mechanisms of adaptation to saline-alkali stress are needed. Most previous studies examining the responses of apple plants to abiotic stress have focused on responses to high temperature, drought, and salt stress [6–8]. The physiological and molecular mechanisms underlying the resistance of apple to saline-alkali stress have not yet been elucidated.

Saline-alkali stress has deleterious effects on the growth and development of plants, as it affects the osmotic balance and increases the pH [9]. The magnitude of damage is greater under saline-alkali stress than under sole salinity stress [10]. Salt stress induces imbalances in concentrations of Na^+ ions, which can disrupt the structure of cells, hinder the transport of other ions, and inhibit growth and energy metabolism [11]. Soil alkaline stress can have effects on various metabolic and physiological processes by altering the extracellular and intracellular pH, including photosynthesis, membrane transport, and reactive oxygen species (ROS) metabolism [12]. Oxidative damage induced by alkaline pH and ion stress can result in the generation of large amounts of ROS in cells, including superoxide anion ($\text{O}_2^{\cdot-}$), hydroxyl ion, hydroxyl radical, and hydrogen peroxide (H_2O_2). This can induce serious damage to the cell membrane, proteins, DNA, and RNA [13].

Among the three types of stress mentioned above, ion stress has the most direct deleterious effects on plants. Several studies have suggested that salt stress can have negative effects on the ability of plants to absorb soil nutrients, and this can inhibit the growth and yield of crops [14]. Soil salinity reduces the uptake of potassium (K), calcium (Ca), and magnesium (Mg) by plants due to ion toxicity and imbalances caused by high Na^+ and Cl^- levels [15,16]. High concentrations of carbonates (CO_3^{2-}) and bicarbonates (HCO_3^-), high pH, and low organic carbon levels also limit the bioavailability of these metals [16]. High bicarbonate concentrations also affect the transport of iron from the cotyledon to the roots in citrus seedlings [17].

The salt overly sensitive (SOS) signaling pathway (including SOS1, SOS2, and SOS3) is activated in plants following exposure to salt stress [18]; the SOS signaling pathway promotes Na^+ efflux to maintain a constant Na^+/K^+ ratio in the cell cytoplasm [19,20]. SOS1, a Na^+/H^+ antiporter protein located on the plasma membrane, regulates Na^+ efflux [21]. Salt stress induces SOS2 activity and its localization to the plasma membrane, which activates the Na^+/H^+ antiporter SOS1 and promotes Na^+ efflux [22]. Cellular ion balance is maintained via the separation of K^+ and Na^+ and mediating their transport into cellular structures such as the vacuoles [23]. A Na^+/H^+ antiporter (NHX) in plant cells mediates the transport of Na^+ into vacuoles, and this protects the cell from being exposed to deleterious ions and ion concentrations [24]. Previous studies have shown that the overexpression of the gene encoding NHX can promote the retention of K^+ , which enhances the salt stress resistance of plants [25].

The various types of injury induced by exposure to saline-alkali stress can promote the accumulation of ROS in plants. ROS function as signaling molecules when they are at low concentrations [26]; however, high concentrations of ROS can have deleterious effects on cell metabolism and inhibit plant growth. Free radical scavenging enzymes and antioxidants are produced in large quantities to mitigate the damage induced by saline-alkali stress [27]. The antioxidant system in plants mainly comprises superoxide dismutase (SOD), peroxidase (POD), catalase (CAT), polyphenol oxidase (PPO), and other enzymes [16]. The accumulation of ROS in plants under saline-alkali stress activates the antioxidant enzyme system, which mitigates the deleterious effects of exposure to salinity and alkalinity and maintains the normal growth of plants [28]. Secondary metabolites such as phenolic compounds also play a role in mediating the clearance of active oxygen as a secondary line of defense under stress [29]. Previous studies have shown that the excessive accumulation of flavonoids promotes antioxidant activity in *Arabidopsis* and enhances its drought resistance [30].

The physiological responses and molecular mechanisms underlying the saline-alkali tolerance of *M. niedzwetzkyana*, a red-fleshed fruit, have not yet been elucidated. In the current study, we compared the resistance of *M. niedzwetzkyana* seedlings and *M. domestica*

“Royal Gala” seedlings to 150 mM saline-alkali stress. RNA-seq was also performed on roots and leaves of *M. niedzwetzkyana* under saline-alkali stress. The aims of this study were as follows: (1) to characterize the tolerance and physiological response of *M. niedzwetzkyana* to saline-alkali stress; (2) to investigate the mechanisms involved in maintaining reactive oxygen species homeostasis, metal ion uptake, and molecular responses to anthocyanoses synthesis under saline-alkali stress; and (3) to identify the key genes related to superoxide dismutase and Na⁺ and K⁺ transport in *M. niedzwetzkyana* under saline-alkali stress.

2. Materials and Methods

2.1. Plant Materials and Saline-Alkali Treatment

Previously preserved wild-type *M. niedzwetzkyana* and wild-type *M. domestica* “Royal Gala” were used in experiments. The plant tissue culture method was used to obtain seedlings of the two apple species. The subculture medium comprised Murashige and Skoog (MS) medium, 0.2 mg/L NAA, and 0.5 mg/L 6-BA. The rooting culture medium comprised 1/2 MS medium and 0.1 mg/L IAA. After growth on the rooting culture medium for 30–40 d, the seedlings were placed in nutrient pots (substrate:vermiculite = 1:1) for cultivation. When the seedlings had 6–8 leaves, 50 seedlings of each apple variety were transferred to Hoagland nutrient solution (pH = 6.0). The seedlings were cultured under hydroponic conditions with 8000–9000 lx artificial lighting for 14 h and a temperature of 24 ± 1 °C. During the experiment, an air compressor was used to aerate the nutrient solution (ventilation period of 30 min with 1 h between each ventilation period). After a pre-cultivation period of 7 d, the seedlings were randomly divided into five groups, including one control group (CK, pH = 6.0) and four treatment groups (pH = 9.0). The nutrient solution used in the treatment group was prepared by mixing NaCl and NaHCO₃ at a molar ratio of 1:1, and the concentration of Na⁺ was 150 mM. Each group had 10 seedlings of two apple varieties. Seedlings in the saline-alkali stress treatment were sampled at 6 h, 12 h, 24 h, and 72 h. The CK group was sampled at 0 h; all other conditions remained unchanged. There were three replicates for each sample, and each replicate consisted of 10 seedlings. The collected leaves and roots were washed with nuclease-free water, immediately frozen in liquid nitrogen, and stored at –80 °C for further experimental analysis.

2.2. Physiological Indexes

Fresh plant samples were snap-frozen in liquid nitrogen for the determination of H₂O₂; O₂²⁻; proline (PRO); and the activities of SOD, POD, CAT, and PPO. The determination of flavonoids, anthocyanins, and Na⁺ and K⁺ content requires dried samples. Dried plant samples are obtained from fresh plant samples by treating them at 105 °C for 30 min and then at 85 °C for 2 h. The content of flavonoids, anthocyanins, H₂O₂, O₂²⁻, and proline (PRO), as well as the activities of SOD, POD, CAT, and PPO, were measured using visible spectrophotometry following the instructions provided in the respective kits (Suzhou Keming Biotechnology Co., Ltd., Suzhou, China). Among them, the superoxide dismutase (SOD) test kit (Item No. SOD-1-W) was selected to measure the SOD activity of the samples using the WST-8 method. The catalase (CAT) test kit (Item No. CAT-2-W) was used to determine the CAT activity of the samples using the ammonium molybdate colorimetric method. The polyphenol oxidase (PPO) kit (Item No. PPO-2-Y) detects the enzyme activity by observing the absorbance change at 525 nm in the reaction system. The peroxidase (POD) kit (Item No. POD-2-Y) detects enzyme activity by monitoring the change of absorbance in 470 nm per minute in the reaction system. The Na⁺ and K⁺ content in the roots was determined using atomic absorption spectrophotometry following the method of Dong et al. [31].

2.3. RNA Extraction and Library Construction

The RNeasy Mini Kit (Qiagen, Germany) was used to isolate total RNA, and this was followed by 1% agarose gel electrophoresis. The integrity of RNA was determined using

an Agilent 2100 bioanalyzer. The NEBNext[®] Ultra[™] Directional RNA Library Prep Kit for Illumina[®] was used to construct libraries. An Illumina NovaSeq 6000 platform (Illumina, Hayward, CA, USA) was used to sequence the libraries.

2.4. Quality Control, Alignment, and Analysis of Sequencing Data

Data were filtered to ensure their quality. This mainly included removing reads with adapters, reads containing N nucleotides, and low-quality reads. The Q20 value, Q30 value, and GC content were calculated for the clean data. High-quality clean data were used in all subsequent analyses. The data quality control results are shown in Table S1.

The Malus reference genome and gene model annotation files were downloaded directly from the National Center for Biotechnology Information (NCBI) URL (accessed on 12 May 2024): https://www.ncbi.nlm.nih.gov/datasets/genome/GCF_002114115.1/. The reference genome index was constructed using HISAT2, and the cleaned paired-end reads were mapped to the reference genome. FeatureCounts was used to determine the number of reads mapped to each gene. The fragments per kilobase per million mapped fragments (FPKM) values for each gene were determined based on its length and the mapped reads.

2.5. Differentially Expressed Gene (DEG), Gene Ontology (GO), and Kyoto Encyclopedia of Genes and Genomes (KEGG) Enrichment Analysis

The DESeq2 package was used to identify DEGs between two comparison groups with adjusted p -values ≤ 0.05 . The significance of DEGs was determined according to the following criteria: corrected p -value < 0.05 and $|\log_2(\text{fold change})| > 1$. The clusterProfiler package version 4.12.0 was used to conduct GO and KEGG pathway enrichment analysis of the DEGs.

2.6. Weighted Gene Co-Expression Network Analysis (WGCNA)

We used the WGCNA package in R software to build weighted gene co-expression networks and identify modules using different expression datasets. We used the “goodSamplesGenes” function to determine whether the sample data were complete, and genes with a missing rate > 0.5 were filtered. We conducted a clustering analysis on the samples using the hclust toolkit (R package version 2.4), and outliers were removed. We used a gradient-independent method, and the “pickSoftThreshold” function was used to select an appropriate soft threshold power (β) between 1 and 30. After determining the power value, the WGCNA algorithm was used to construct modules, and a topological overlap matrix was built using expression values. The “dynamicTreeCut” algorithm was used to detect modules (Langfelder and Horvath, 2008). After the association of each module with sample phenotypes was determined, the most relevant module was selected for subsequent analysis. We predicted the subcellular localization of potential candidate metal ion transporters using the online website Plant-mPLOC URL (accessed on 12 May 2024): <http://www.csbio.sjtu.edu.cn/bioinf/plant-multi/> [32].

2.7. Quantitative Reverse Transcription Polymerase Chain Reaction (RT-qPCR) Validation of RNA Sequencing (RNA-Seq) Data

RT-qPCR was used to verify the expression levels of candidate DEGs inferred from the transcriptome data. Premier 6 software was used to design specific primers. cDNA synthesis and RT-qPCR analysis were conducted following the methods described in a previous study [4]. The primers used for RT-qPCR are shown in Table S3.

2.8. Data Accessibility

The supporting dataset is included in this study and the Supplementary Materials. The reads generated in this study were submitted to the Sequence Read Archive at the NCBI under accession number PRJNA1047940. The dataset can be accessed at the following URL (accessed on 12 May 2024): <http://www.ncbi.nlm.nih.gov/sra/>.

2.9. Statistical Analysis

All data in this experiment were analyzed and processed for data analysis and graphing using Microsoft Office 16 Excel (Microsoft, Seattle, WA, USA). GraphPad Prism 6 (GraphPad Software, La Jolla, CA, USA) was used for graphing, ANOVA, and *t*-tests. Each bar represents the mean \pm standard error (SE) of at least three replicates.

3. Results

3.1. Phenotypic Changes under Saline-Alkali Treatment

To determine whether *M. niedzwetzkyana* has strong saline-alkali tolerance, Red (*M. niedzwetzkyana*) seedlings and Gala (*M. domestica* "Royal Gala") seedlings were placed in a high-pH Hoagland nutrient solution containing NaCl and NaHCO₃. The saline-alkali tolerance of Red plants was greater than that of Gala plants under 72 h of saline-alkali treatment. Wilting was observed in both Gala and Red plants after exposure to saline-alkali treatment for 72 h, but wilting was more severe in Gala plants than in Red plants (Figure 1A). The anthocyanin content was higher in Red leaves than in Gala leaves (Figure 1B). The difference in the anthocyanin content between the two species of plants increased after saline-alkali treatment. The flavonoid content in the leaves of both plant species remained the same in the control group throughout the experimental period. The flavonoid content in Red leaves was higher than that in Gala leaves at 6 h of treatment; however, the flavonoid content was higher in Gala leaves than in Red leaves after 72 h (Figure 1C).

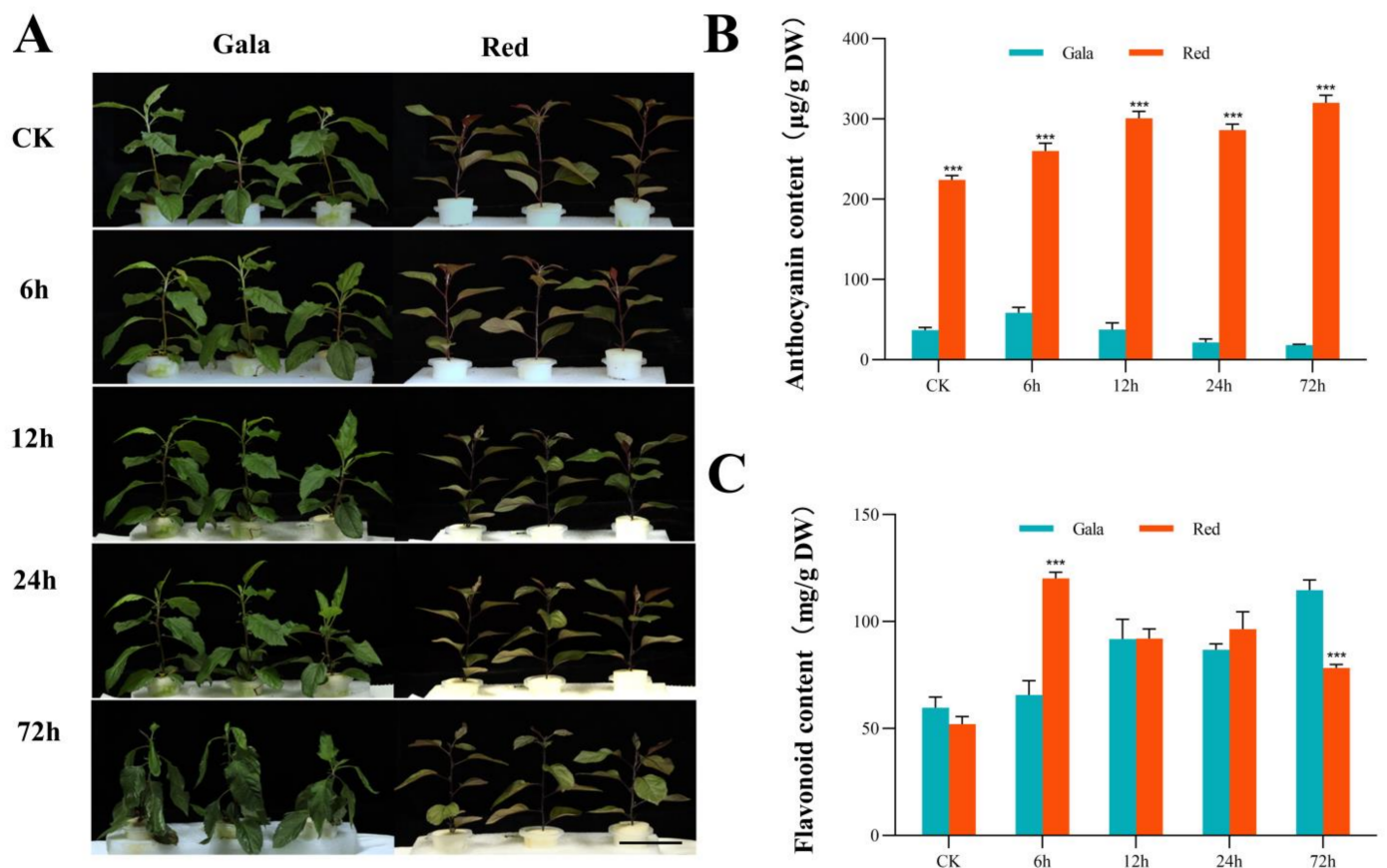


Figure 1. Morphological changes of *M. niedzwetzkyana* and *M. domestica* "Royal Gala" seedlings treated with 150 mM saline-alkali stress (Gala: *M. domestica* "Royal Gala", Red: *M. niedzwetzkyana*). (A) Phenotype, bar = 5 cm; (B) leaf anthocyanin content; and (C) leaf flavonoid content. Thresholds for statistical significance according to *t*-tests: *** $p < 0.01$. The *x*-axis shows the processing time, and the *y*-axis shows measurement indexes.

3.2. Activity of Antioxidant Enzymes under Saline-Alkali Treatment

Significant changes were observed in the content of H_2O_2 in the two apple plants under saline-alkali stress (Figure 2). The H_2O_2 content was lower in Red plants than in Gala plants at 12 h, which indicates that the antioxidant capacity was higher in Red plants than in Gala plants (Figure 2A). In addition, we compared the activity of antioxidant enzymes (POD, SOD, CAT, and PPO) in leaves under normal conditions and saline-alkali stress at different times. Under normal conditions, PPO activity was higher in Red leaves than in Gala leaves. Following exposure to saline-alkali stress for 72 h, the activity of SOD, POD, CAT, and PPO was significantly higher in Red leaves than in Gala leaves. The CAT activity markedly increased in Red leaves at 12 h, and this was consistent with the observed changes in the H_2O_2 content (Figure 2A,E). These findings suggest that 150 mM saline-alkali treatment induced strong oxidative stress in the two apple plant species, and the antioxidant capacity of Red leaves was higher than that of Gala leaves.

3.3. Metal Ion and PRO Content under Saline-Alkali Treatment

To clarify the response of Red plants to ionic stress and osmotic stress, we measured the content of Na^+ and K^+ ions in the root system and the PRO content in the leaves at different time points (Figure 3). Changes in the Na^+ and K^+ content in the roots of Red plants were varied. In the early part of the experimental period, the content of Na^+ was lower in the roots of Red plants than in Gala plants; the Na^+/K^+ ratio in Red plants was one-third of that in Gala plants at 6 h (Figure 3C). The PRO content was slightly lower in Red leaves than in Gala leaves in the early part of the experimental period; however, the PRO content was higher in Gala leaves than in Red leaves in the latter part of the experimental period (Figure 3D). This might stem from the fact that the magnitude of the damage induced by saline-alkali stress was lower in Red plants than in Gala plants early in the experimental period.

3.4. RNA-Seq Analysis

Significant increases in the content of flavonoids, antioxidant enzymes, and ions were observed in Red leaves and roots at 6 h and 12 h. Therefore, the signaling pathways involved in the response to saline-alkali stress in *M. niedzwetzkyana* were identified by sequencing leaf and root samples collected at 0 h, 6 h, and 12 h. We constructed 18 RNA-seq strand-specific libraries and sequenced them; three replicates were performed for each sample. The transcriptome of *M. niedzwetzkyana* under saline-alkali treatment was obtained. After removing low-quality reads and adapter sequences, we obtained 781,306,798 clean reads and 117.21 G clean bases; the average GC content was 46.43%. The sequencing error rate for each sample was 0.03%, and the average Q20 and Q30 values were 97.39% and 92.60%, respectively (Table S1). According to the FPKM values of all genes in each sample, we calculated the correlation coefficients within and between groups and made a heat map. The R^2 values of almost all samples were >0.9 (Figure S1), and significant differences were observed between leaf and root samples. This suggests that the experimental data collected were robust and that they could be used in subsequent analyses.

3.5. DEGs Involved in the Response to Saline-Alkali Stress

DEGs between libraries were considered significant using DESeq2 according to the following criteria: $|\log_2(\text{fold change})| > 1$ and $\text{padj} < 0.05$. Pairwise comparisons of DEGs among the three time points were made, and scatter plots of the number of up-regulated and down-regulated genes between tissues are shown in Figure 4A. The number of down-regulated genes was higher than the number of up-regulated genes in both the leaves and roots under saline-alkali stress compared with the control. However, comparison of samples from 6 h and 12 h revealed that the number of up-regulated genes was slightly higher than the number of down-regulated genes, which indicates that a greater number of signaling pathways were activated in the leaves and roots as the treatment time increased. Overall, the number of up-regulated and down-regulated DEGs was greater in the roots

than in the leaves; specifically, the expression of 4302 genes was up-regulated in R12h (group 5), and the expression of only 2938 genes was down-regulated (group 1). These findings indicate that the response of the roots to saline-alkali stress might be stronger than the response of the leaves to saline-alkali stress. The number of DEGs increased with the treatment duration.

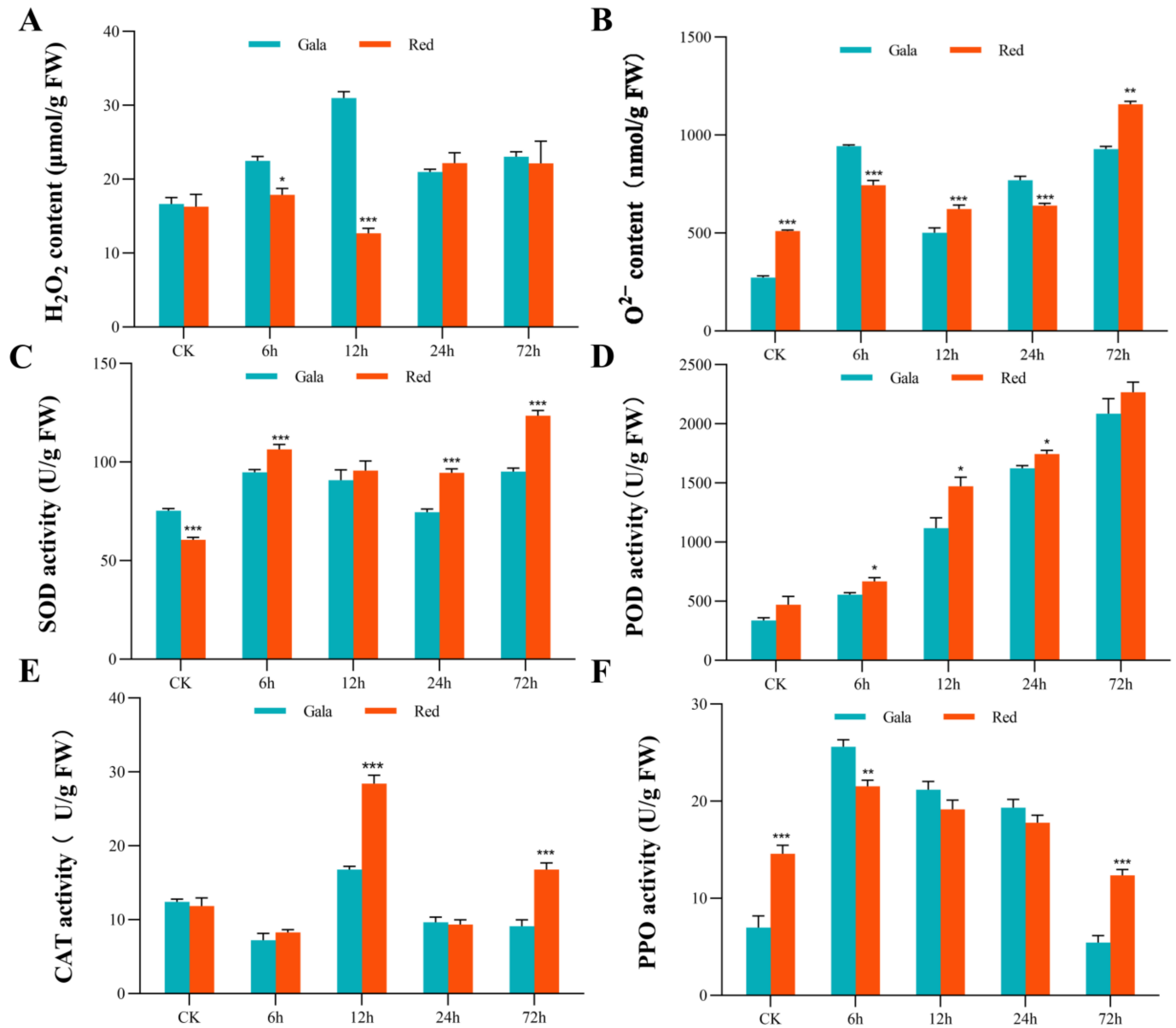


Figure 2. Changes in the activity of leaf enzymes of *M. niedzwetzkyana* and *M. domestica* “Royal Gala” seedlings treated with 150 mM saline-alkali stress. (A) H₂O₂ content, (B) O₂⁻ content, (C) SOD activity, (D) POD activity, (E) CAT activity, and (F) PPO activity. Thresholds for statistical significance according to *t*-tests: *** *p* < 0.01; ** *p* < 0.01–0.05; and * *p* < 0.1–0.05. The *x*-axis shows the processing time, and the *y*-axis shows the measurement indexes.

Venn diagrams are effective for visualizing shared and unique genes between samples, and they facilitate the identification of key DEGs. A total of 8292 DEGs involved in the response to saline-alkali stress in the leaves were identified at 6 h and 12 h, and a total of 11,871 DEGs involved in the response to saline-alkali stress in the roots were identified at the same time points (Figure 4B). A total of 4033 shared DEGs involved in the response to saline-alkali stress were identified in both the roots and leaves. Venn analysis revealed 599 differentially co-expressed genes in the roots and leaves that were involved in the

response to saline-alkali stress at both 6 h and 12 h (Figure 4C). These differentially co-expressed genes might play various roles in the response to saline-alkali stress.

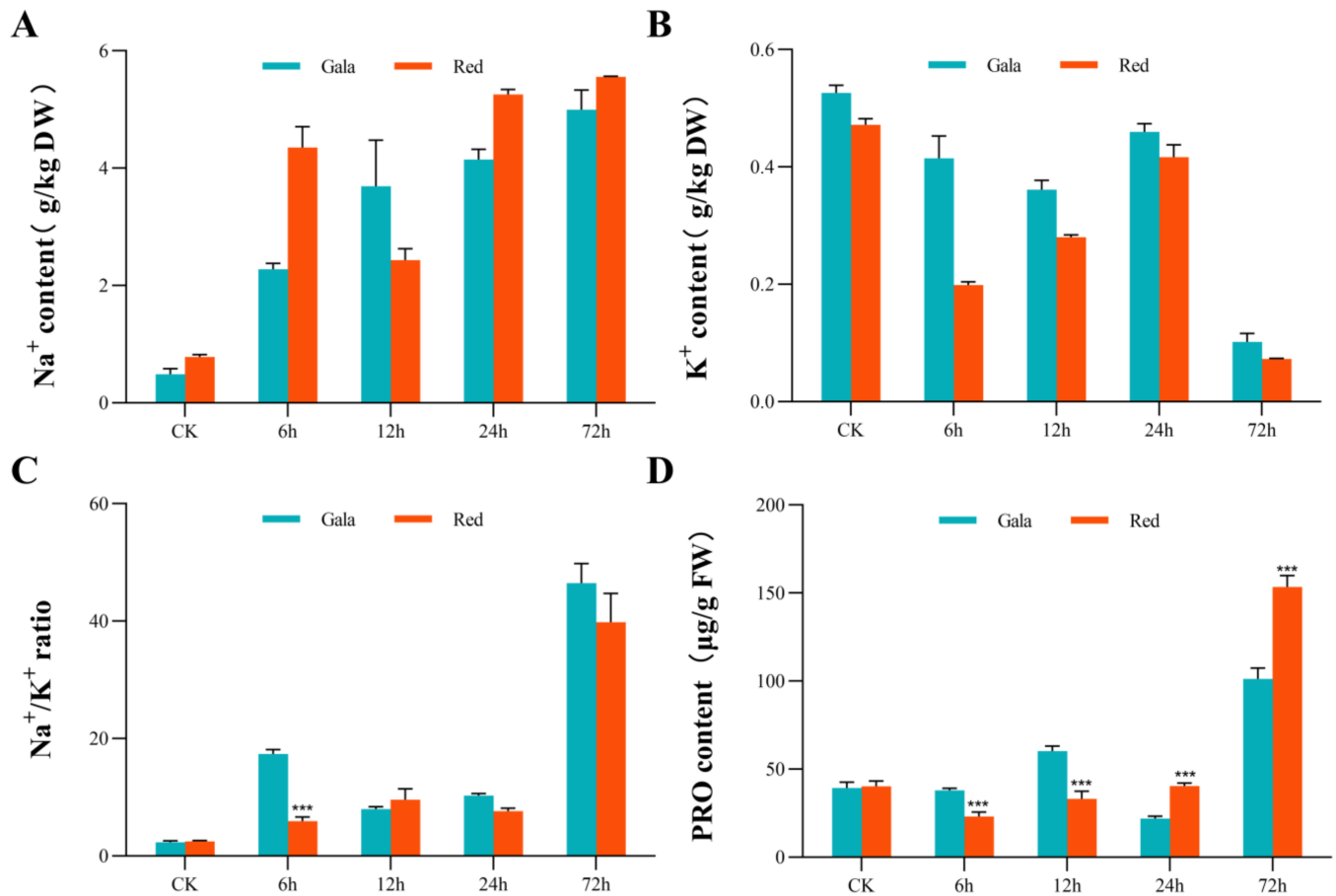


Figure 3. Changes in the root Na^+/K^+ content and leaf PRO content of *M. niedzwetzkyana* and *M. domestica* “Royal Gala” seedlings under 150 mM saline-alkali treatment. (A) Root Na^+ content, (B) root K^+ content, (C) root K^+/Na^+ ratio, and (D) leaf PRO content. Thresholds for statistical significance according to *t*-tests: *** $p < 0.01$. The *x*-axis shows the processing time, and the *y*-axis shows the measurement indexes.

3.6. GO Analysis of DEGs Involved in Saline-Alkali Stress

To clarify the roles of DEGs in the response to saline-alkali stress, we conducted a GO analysis of DEGs. GO terms were divided into three categories: molecular function (MF), cellular component (CC), and biological process (BP) (Tables 1 and 2). We detected significant differences in the enriched GO terms between the leaves and roots; only GO terms in the MF category were enriched in leaves. Other GO terms in the MF category that were significantly enriched included tetrapyrrole binding, heme binding, iron ion binding, oxidoreductase activity, and hydrolase activity. In the CC category, significantly enriched GO terms in the roots included cell periphery, extracellular region, cell wall, external encapsulating structure, and apoplast at 6 h and 12 h. In the BP category, significantly enriched GO terms in the roots included cellular carbohydrate metabolic process, defense response, and cellular polysaccharide metabolic process. This suggests that the response of the root system to saline-alkali stress is particularly strong, and metal ion proteins might play a key role in this process.

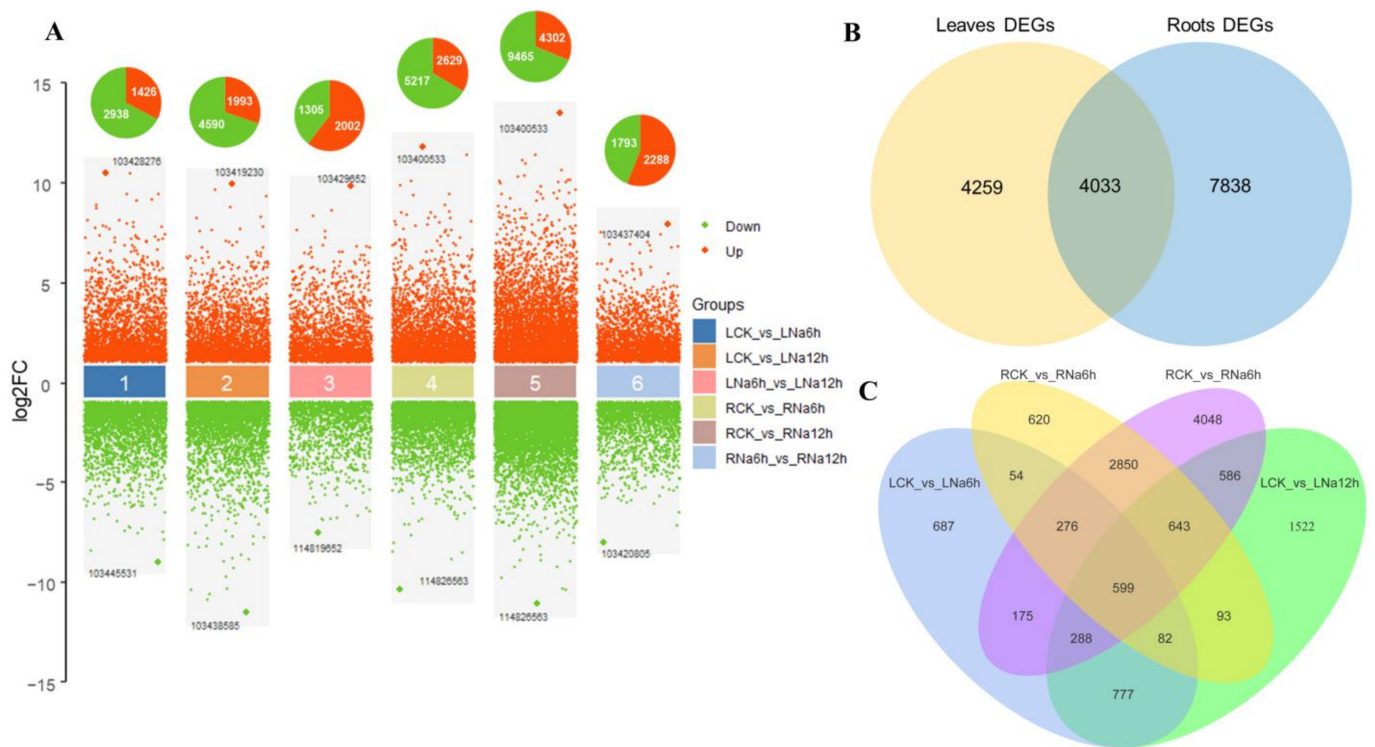


Figure 4. Analysis of DEGs between treatments and the control. (A) Multiple scatter plots of the DEGs. The y-axis shows the Log₂ (fold change). The red dots indicate up-regulated genes, and green dots indicate down-regulated genes. (B) All common DEGs in the roots and leaves. (C) Specific and common DEGs among treatments in the Venn diagrams.

Table 1. GO enrichment analysis of the consistent DEGs in leaves.

GO ID	GO Name	Category	LCK vs. LNa6h DEGs Number	LCK vs. LNa12h DEGs Number
GO:0016757	transferase activity, transferring glycosyl groups	MF	34	51
GO:0016758	transferase activity, transferring hexosyl groups	MF	30	46
GO:0020037	heme binding	MF	31	40
GO:0046906	tetrapyrrole binding	MF	31	40
GO:0005506	iron ion binding	MF	33	34
GO:0016705	oxidoreductase activity, acting on paired donors, with incorporation or reduction of molecular oxygen	MF	28	30
GO:0016798	hydrolase activity, acting on glycosyl bonds	MF	15	20
GO:0004553	hydrolase activity, hydrolyzing O-glycosyl compounds	MF	13	20
GO:0000155	phosphorelay sensor kinase activity	MF	1	2
GO:0004673	protein histidine kinase activity	MF	1	2
GO:0016775	phosphotransferase activity, nitrogenous group as acceptor	MF	1	2

(MF: molecular function).

3.7. KEGG Pathway Enrichment Analysis of DEGs Involved in Saline-Alkali Stress

We conducted a KEGG pathway enrichment analysis of DEGs to identify the main metabolic pathways involved in resistance to saline-alkali stress. A total of 21 KEGG pathways were identified in the leaves and roots under saline-alkali stress (Tables 3 and 4). Consistent with the GO enrichment results, the number of enriched pathways was greater in the roots than in the leaves. The glutathione metabolism was the only pathway enriched in both the roots and leaves. The metabolic pathways enriched in the roots mainly included ABC transporters, plant hormone signal transduction, phenylpropanoid biosynthesis, flavonoid biosynthesis, and cysteine and methionine metabolism. These findings suggest

that resistance to saline-alkali stress in the roots is achieved by regulating the synthesis of plant hormones and secondary metabolites.

Table 2. GO enrichment analysis of the consistent DEGs in roots.

GO ID	GO Name	Category	RCK vs. RNA6h DEGs Number	RCK vs. RNA12h DEGs Number
GO:0016758	coenzyme binding	MF	100	156
GO:0015267	tetrapyrrole binding	MF	40	188
GO:0046527	heme binding	MF	28	188
GO:0003777	hydrolase activity, acting on glycosyl bonds	MF	43	161
GO:0015631	hydrolase activity, hydrolyzing O-glycosyl compounds	MF	47	151
GO:0008017	iron ion binding	MF	47	148
GO:0060089	transferase activity, transferring hexosyl groups	MF	21	172
GO:0005507	oxidoreductase activity, acting on paired donors, with incorporation or reduction of molecular oxygen	MF	27	158
GO:0004553	passive transmembrane transporter activity	MF	91	61
GO:0050662	copper ion binding	MF	101	41
GO:0071944	cell periphery	CC	25	39
GO:0005576	extracellular region	CC	20	25
GO:0005618	cell wall	CC	16	20
GO:0030312	external encapsulating structure	CC	16	20
GO:0048046	apoplast	CC	16	20
GO:0006073	cellular carbohydrate metabolic process	BP	26	64
GO:0006928	defense response	BP	43	41
GO:0006952	reproduction	BP	32	49
GO:0051704	reproductive process	BP	32	49
GO:0006270	microtubule-based process	BP	11	68
GO:0044262	cellular polysaccharide metabolic process	BP	39	40
GO:0008037	pollination	BP	30	47
GO:0009856	pollen-pistil interaction	BP	30	47
GO:0009875	multi-multicellular organism process	BP	30	47
GO:0044706	recognition of pollen	BP	30	47
GO:0044042	multi-organism process	BP	26	50
GO:0044264	cell recognition	BP	26	47

(MF: molecular function, CC: cellular component, BP: biological process).

Table 3. KEGG enrichment analysis of the DEGs in leaves.

KEGGID	KEGG Pathway	LCK vs. LNa6h DEGs Number	LCK vs. LNa12h DEGs Number
mdm00480	Glutathione metabolism	30	34
mdm00500	Starch and sucrose metabolism	33	50
mdm00630	Glyoxylate and dicarboxylate metabolism	21	28
mdm00906	Carotenoid biosynthesis	13	18
mdm04712	Circadian rhythm—plant	21	30
mdm01200	Carbon metabolism	56	92

3.8. DEGs Involved in the Anthocyanin Synthesis Pathway Mediate the Response to Saline-Alkali Stress

KEGG pathway enrichment analysis revealed that phenylpropanoid and flavonoid biosynthesis played a role in the response to saline-alkali stress, and these are associated with the anthocyanin synthesis pathway. The content of anthocyanins is high in *M. niedzwetzkyana*. Thus, we built a heat map of the anthocyanin metabolic pathway to analyze changes in related DEGs (Figure 5). In phenylpropanoid biosynthesis, the expression of most DEGs in the roots and leaves was up-regulated following exposure to saline-alkali stress, and this provides ample raw materials for the synthesis of flavonoids. However, in

the anthocyanin synthesis pathway, the expression of most genes in the roots and leaves was down-regulated following exposure to saline-alkali stress. The expression of CHS, F3H, DRF, ANS, and UFGT was down-regulated after 6 h and 12 h of saline-alkali treatment. The expression of a copy of *MdCHI* (LOC103421113) was up-regulated following exposure to saline-alkali stress, and it was highly expressed in the roots. This might explain why *M. niedzwetzkyana* shows high saline-alkali resistance.

Table 4. KEGG enrichment analysis of the DEGs in roots.

KEGGID	KEGG Pathway	RCK vs. RNA6h DEGs Number	RCK vs. RNA12h DEGs Number
mdm00040	Pentose and glucuronate interconversions	27	43
mdm00270	Cysteine and methionine metabolism	41	65
mdm00350	Tyrosine metabolism	18	29
mdm00430	Taurine and hypotaurine metabolism	8	11
mdm00460	Cyanoamino acid metabolism	23	29
mdm00480	Glutathione metabolism	41	63
mdm00592	alpha-Linolenic acid metabolism	22	38
mdm00910	Nitrogen metabolism	16	28
mdm00940	Phenylpropanoid biosynthesis	63	103
mdm00941	Flavonoid biosynthesis	30	49
mdm00950	Isoquinoline alkaloid biosynthesis	10	15
mdm00960	Tropane, piperidine, and pyridine alkaloid biosynthesis	15	21
mdm02010	ABC transporters	30	38
mdm03030	DNA replication	19	34
mdm04075	Plant hormone signal transduction	75	122

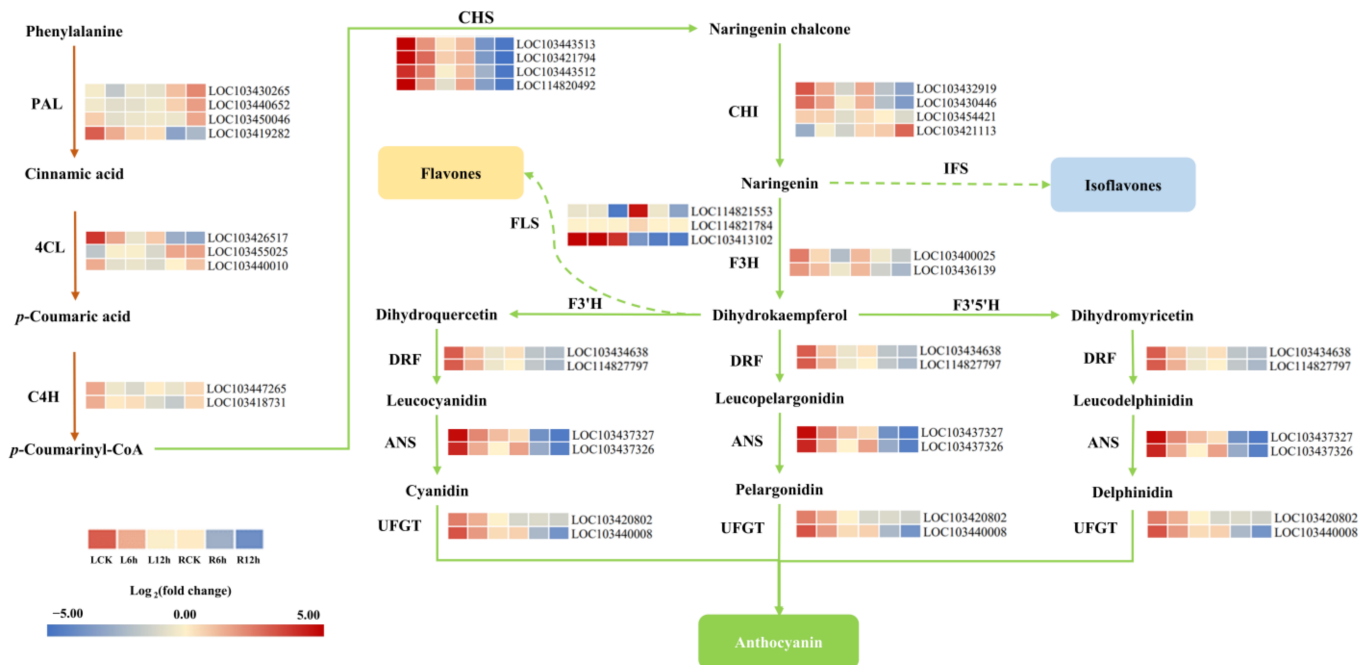


Figure 5. Anthocyanin metabolism responses to saline-alkali stress in *M. niedzwetzkyana* and the DEG heat map. The relative expression levels of DEGs were calculated using the Log_2 ratio. The LCK group was used as the control group.

3.9. DEGs Encoding Antioxidant Enzymes Involved in the Response to Saline-Alkali Stress

According to measurements of physiological indexes, the antioxidant capacity of *M. niedzwetzkyana* was strong. We determined the core antioxidant genes through anal-

ysis of the expression levels of DEGs encoding antioxidant enzymes. We identified 41 differentially expressed antioxidant enzyme genes (Figure 6). SODs can be divided into three types according to their metal cofactors, Cu/Zn-SODs, Mn-SODs, and Fe-SODs, and Cu/Zn-SODs are specific to eukaryotes [27]. We identified four Fe-SODs and two Cu/Zn-SODs under saline-alkali stress. The expression of two Cu/Zn-SOD genes (LOC103413973, LOC103450984) was up-regulated following exposure to saline-alkali stress, and the expression of Fe-SOD2a (LOC103420753) was down-regulated in the leaves and roots under normal conditions. We identified 26 POD genes and two CAT genes. The expression of *MdCAT1* (LOC103436733) and *MdCAT1Like* (LOC103445262) was higher under saline-alkali stress than in the control, but they exhibited opposite expression patterns. The expression of *MdCAT1Like* was up-regulated following 6 h and 12 h of saline-alkali stress, and the fold change was higher at 6 h than at 12 h. This was strongly correlated with changes in leaf CAT activity. We also identified four PPO genes. The expression of *MdPPO* (LOC103446446) was low in the leaves and high in the roots, and it responded strongly to saline-alkali stress. The previously collected physiological data and analysis of DEGs encoding antioxidant enzymes revealed that the expression of antioxidant genes was significantly up-regulated in the roots of *M. niedzwetzkyana* to maintain the intracellular ROS balance during saline-alkali stress, which enhanced adaptation and resistance to saline-alkali stress.

3.10. Ion Transporters in Response to Saline-Alkali Stress in DEGs

Ion transporters play key roles in mediating the absorption, transport, and chelation of Na^+ and K^+ . We analyzed the DEGs encoding ion transporters. Following exposure to saline-alkali stress, we found that the expression of *MdCHX20L* (LOC103433392), *MdKEA5* (LOC103439647), and *MdMHX* (LOC103432597) was up-regulated in both the root and leaf tissues, and the expression of *MdKEA2* (LOC103439264) was down-regulated in both root and leaf tissues. The expression of a large number of Ca^{2+} /cation antiporter genes increased in the leaves; the expression of these genes in the roots was weak. This suggests that CaCA family members play an important role in maintaining the ionic balance of leaves, and the several CAX proteins identified might mediate the transport of various cations (Figure 7A). Finally, we predicted the cellular localization of these ion transporters online using Plant-mPLOC. The predicted results are shown in a cytoarchitectural map (Figure 7B).

3.11. WGCNA

We constructed a co-expression module with 38,554 genes expressed in 18 samples using the WGCNA tool. The sample dendrogram and heat map are shown in Figure 8A. According to the independence criterion of 0.9, the suitable power value was determined to be 24. This power value was then used to create co-expression modules. To correlate the modules with sample traits, we once again determined the antioxidant enzyme activity and metal ion content for 18 samples (Table S2). These modules are shown in various colors in Figure 8B. We examined interactions between these co-expression modules. The correlations between the module eigengene and traits are shown in Figure 8A. Both green and turquoise modules were significantly associated with antioxidant activity and the metal ion content. We defined gene significance (GS) as the absolute value of the correlation between genes and traits and module membership (MM) as the correlation between the eigengene of a module and the gene expression profile. The GS and MM coefficients of the green and turquoise modules were calculated based on the SOD activity and Na and K content, respectively. A scatter plot was made, and genes with GS and MM greater than 0.8 in the module were selected as candidate genes (Figure 9). Further analysis of the candidate genes revealed several core genes, such as *MdWRKY1Like* (LOC103404995), *MdCIPK19* (LOC103422372), *MdbHLH80Like* (LOC103425311), *MdPP2C39* (LOC103448709), and *MdMYB5Like* (LOC103455783).

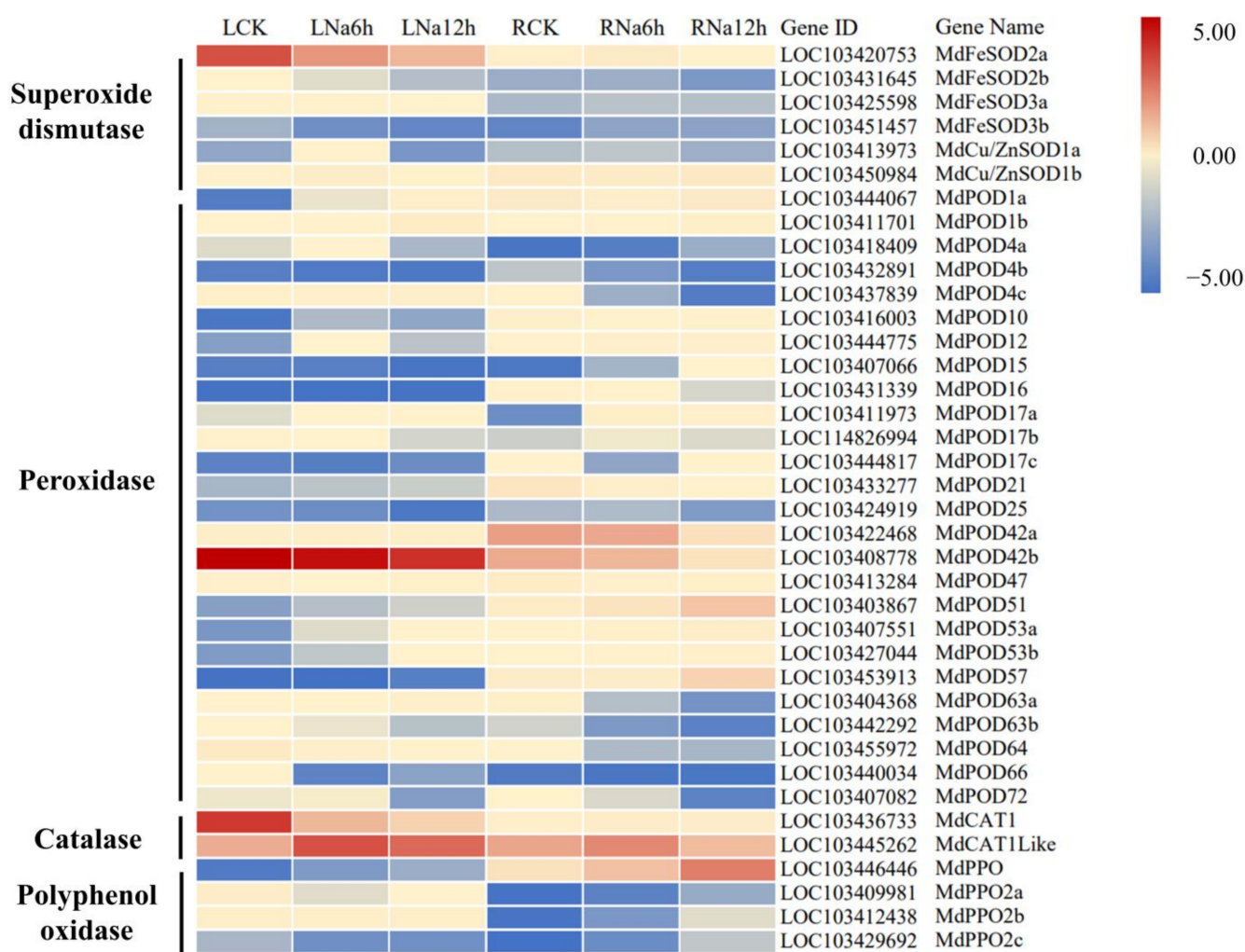


Figure 6. Heat map of antioxidant enzyme DEGs involved in the response to saline-alkali stress. The relative expression levels of DEGs were calculated using the Log₂ ratio. The LCK group was used as the control group.

3.12. RT-qPCR Validation of Candidate Genes

To validate the gene expression patterns inferred from the RNA-Seq analysis, we conducted an RT-qPCR analysis of candidate genes encoding selected TFs, calmodulins, and phosphorylase kinases (Figure 10). The selected TFs included four WKRY genes, two MYB genes, one NAC gene, and one BHLH gene. We found that the FPKM values of the selected TFs were strongly correlated with the expression levels obtained from RT-qPCR. The expression of these TFs was up-regulated to varying degrees by saline-alkali stress as the treatment time increased. This indicates that the expression of these TFs might be positively correlated with the degree of saline-alkali tolerance of the plants. We also identified two proteins from the PP2C family: *MdPP2C29Like* (LOC103416868) had low expression in the leaves and gradually increasing expression in the roots, and *MdPP2C39* (LOC103448709) had high and increasing expression in the leaves but the expression was decreasing in the roots. We also found that a CML gene and CIPK gene played a role in the response to saline-alkali stress. These findings suggest that *M. niedzwetzkyana* tolerates saline-alkali stress by inducing the expression of related TFs and protein kinases. These genes are strongly correlated with SOD activity and the content of Na⁺ and K⁺ ions; these data provide new insights into the signaling pathways underlying saline-alkali stress in apple.

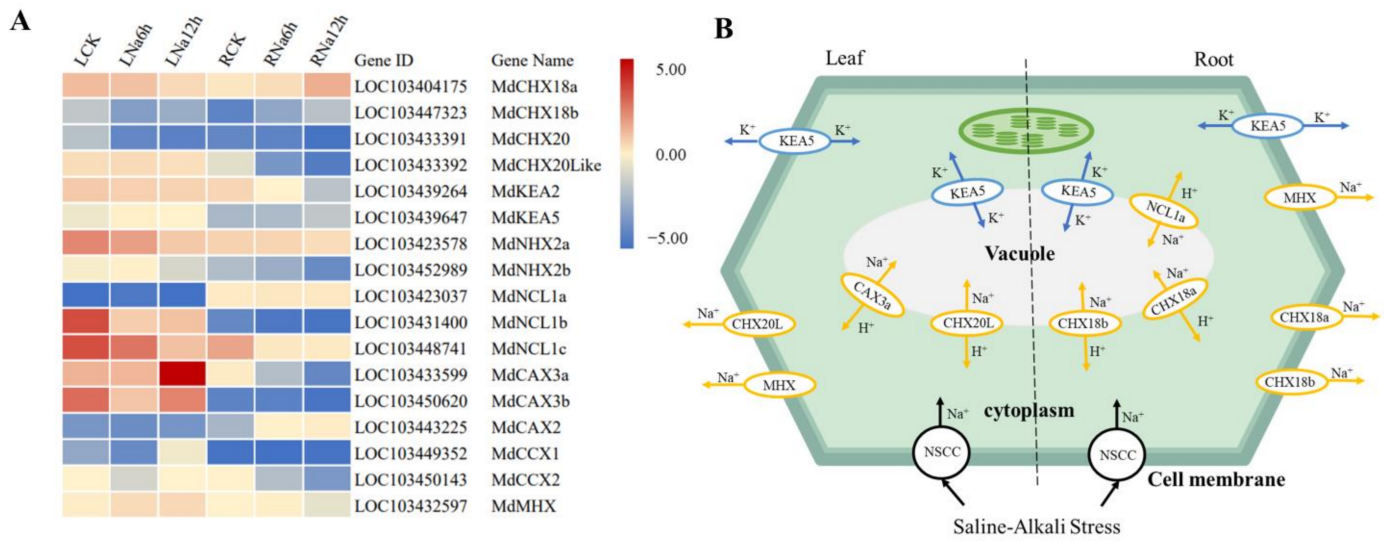


Figure 7. DEGs encoding ion transporters in response to saline-alkali stress. **(A)** Heat map of ion transporters in DEGs. The relative expression levels of DEGs were calculated using the Log₂ ratio. LCK group was used as control group. **(B)** Saline-alkali ion transport model in the roots and leaves. The direction of the arrows in the model is the direction of metal ion transport. Black arrows represent passive transport of Na⁺, blue arrows represent active transport of K⁺, yellow arrows represent active transport of Na⁺/H⁺.

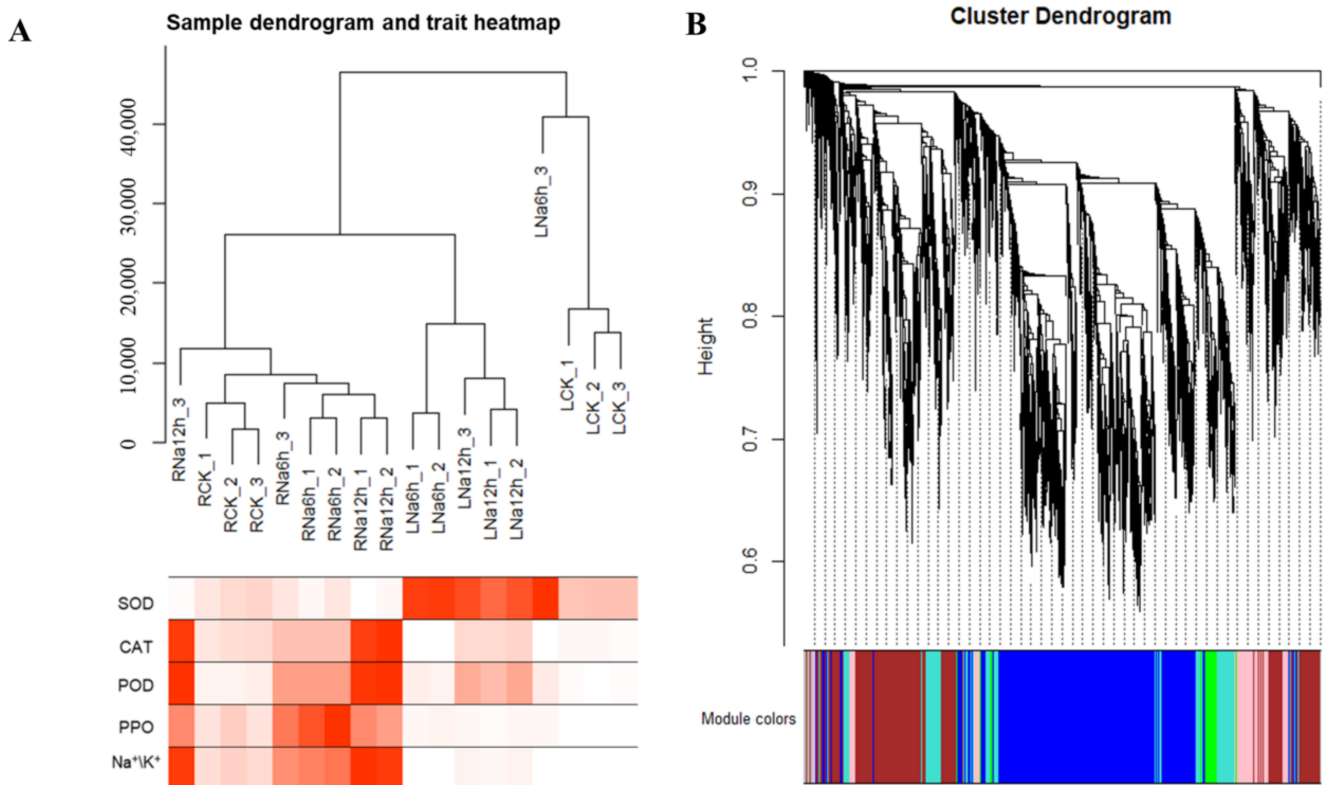


Figure 8. WGCNA. **(A)** Sample dendrogram and trait heat map of 18 samples. **(B)** Clustering dendrogram, with dissimilarity based on the topological overlap, along with the assigned module colors. Each branch corresponds to different modules, and each line corresponds to one gene.

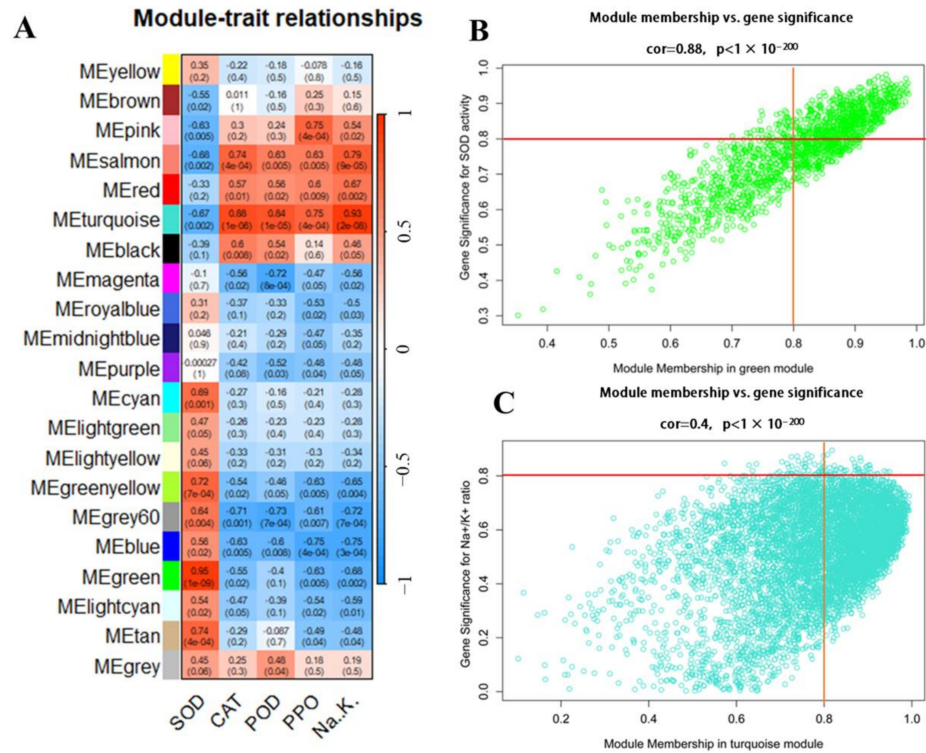


Figure 9. Associations between modules and sample traits. (A) Module–trait relationships. (B) Scatter plots of GS and MM for SOD activity in the green module. (C) Scatter plots of GS and MM for the Na and K content in the turquoise module. GS: gene significance; MM: module membership.

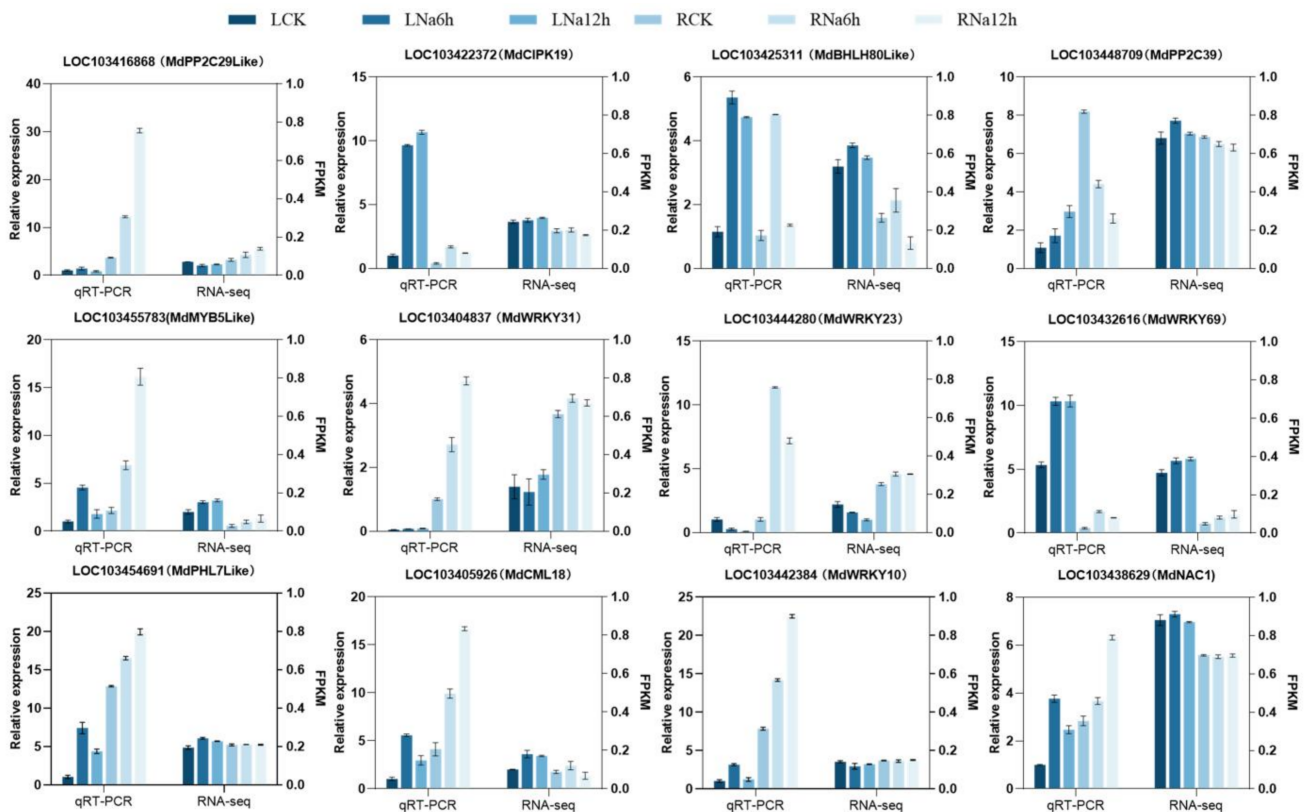


Figure 10. RT-qPCR validation of hub genes in *M. niedzwetzkyana* after the roots and leaves were subjected to saline-alkali stress for 6 h and 12 h. Data from RT-qPCR are mean ± SE (n = 3). Data from RNA-seq are the mean of three replicates and were log₂-transformed.

4. Discussion

Saline-alkali stress is a complex stress that can disrupt the structure of plant cells, accelerate the generation of ROS, induce damage to plants, and disrupt metabolic pathways [33,34]. Transcriptional regulation, morphophysiological responses, and biochemical metabolic processes play key roles in the responses of plants to environmental stimuli [35]. Several studies have focused on the perception and transcriptional regulatory mechanisms of saline-alkali signals in model plants and major crops [36]. The study of wild species and plants with high saline-alkali tolerance is critically important for elucidating the molecular basis of saline-alkali tolerance and identifying candidate genes for crop improvement. *M. niedzwetzkyana* is a wild apple resource with a long evolutionary history [5]; it has developed a unique red flesh and mechanisms to adapt to saline-alkali conditions [4]. We thus examined the molecular mechanisms underlying the response to saline-alkali stress; generally, identifying new stress-resistant genes is critically important for enhancing the resistance of crops to saline-alkali stress.

The high anthocyanin content of *M. niedzwetzkyana* confers it with a red phenotype. Thus, we were particularly interested in the response of the anthocyanin synthesis pathway to saline-alkali stress. We used *M. domestica* "Royal Gala" as a reference to evaluate the saline-alkali resistance of *M. niedzwetzkyana*. Physiological data suggest that saline-alkali stress affects the metabolism of phenolic compounds in apple leaves. We investigated changes in the anthocyanin synthesis pathway at the transcriptional level. Under saline-alkali stress, the expression of the genes involved in the synthesis of flavonoid anthocyanins in *M. niedzwetzkyana* was down-regulated, and the expression of only one *CHI* gene was up-regulated. However, physiological data show that anthocyanin levels are not stable. This indicates that the effect of saline-alkali stress on anthocyanin synthesis is complex and cannot be fully characterized at the transcriptional level. *CHI* functions as the second rate-limiting enzyme and is the first enzyme involved in the biosynthesis of flavonoids [37]. Research on *CHI* in *Arabidopsis thaliana* has confirmed that it plays a unique positive role in the flavonoid pathway [38]. We speculate that the unique response of *MdCHI* to saline-alkali stress might explain the increase in the content of total flavonoids in *M. niedzwetzkyana* leaves after 6 h. However, the high flavonoid content of *M. niedzwetzkyana* plays a role in saline-alkali stress resistance, and its ability to resist stress is associated with the action of the antioxidant enzyme system and ion transporter proteins.

The negative effects of saline-alkali stress on plants mainly stem from the high pH, which leads to the excessive production of ROS. Plants with strong antioxidant capabilities that rapidly respond to oxidative stress are typically resistant to non-biotic and biotic stresses [39,40]. High antioxidant capabilities allow plants to adapt to adverse environments and improve their stress tolerance [39]. The antioxidant system of plants is activated under saline-alkali stress, and the activity of antioxidant enzymes mitigates the deleterious effects of saline-alkali stress. Under saline-alkali stress, the activities of SOD, POD, and CAT in *M. niedzwetzkyana* leaves significantly increased. The expression of many DEGs involved in redox processes was significantly enriched under saline-alkali stress. Following exposure to saline-alkali stress, several antioxidant genes were detected in *M. niedzwetzkyana*, and one highly expressed polyphenol oxidase gene (*PPO*) was particularly noteworthy. *PPO* is a ubiquitous protein expressed in many organs; it is involved in fruit enzymatic browning and can be induced by stress [41]. *MnMYB3R* in *Morus notabilis* Schneid up-regulates the expression of *NtPPO1*, which is homologous to *MnPPO2*, and *PPO* activity was induced in response to drought stress after it was heterologously expressed in tobacco [42]. However, the mechanism underlying the response of *PPO* to saline-alkali stress has not yet been elucidated. In this study, we measured the *PPO* activity in leaves and found that *PPO* strongly responds to saline-alkali stress, and the content of *PPO* was higher in highly resistant varieties. The activity of CAT in *M. niedzwetzkyana* significantly increased by 12 h following exposure to saline-alkali treatment, and the content of H_2O_2 decreased significantly at 12 h, indicating that this finding is not a product of experimental error. We identified the DEG *MdCAT1Like* (*LOC103445262*), and its expression was up-regulated

2.29-fold and 1.95-fold in the leaves following exposure to 6 h and 12 h of saline-alkali treatment, respectively. Previous studies have shown that activation of the CAT-dependent redox homeostasis pathways can enhance the tolerance of tea plants to salt stress, and this was also confirmed in our study.

Examining the exchange of water and ions is key to studies of salt stress responses [43]. In salt-tolerant plants, the absorption, transport, and separation of inorganic ions as osmotic regulators are effective methods for alleviating osmotic stress [44]. Most salt-tolerant plants employ strategies to prevent the excessive influx of Na^+ into cells, accelerate Na^+ efflux, and increase K^+ uptake to reduce salt-induced damage [45]. The Na^+/K^+ ratio is commonly used as an indicator of the degree to which the ionic balance is disrupted by salt stress, and a lower ratio indicates high salt tolerance [46]. In our study, the root Na^+/K^+ ratio in *M. niedzwetzkyana* was significantly lower than that in Gala, suggesting that the root system of *M. niedzwetzkyana* maintains active cellular uptake of K^+ while resisting invasion by high Na^+ concentrations. This enhances the resistance of the roots to osmotic stress caused by salt stress.

Several studies of the functions of transporters under adverse conditions have been conducted. For example, *MdNHX1* overexpression significantly enhances salt resistance in apple callus cells and Arabidopsis [47]. Overexpression of the vacuolar Na^+/H^+ antiporter *MdNHX2* confers salt tolerance in apple rootstock M26 [48]. The presence of *MdCCX1*, an ion/ Ca^{2+} exchanger in the plasma membrane, slows the accumulation of ions and ROS, thereby enhancing plant tolerance to salt stress [36]. In the transcriptome, we screened a large number of ion transporters, mainly members of the NHX and CCX families, which is consistent with the results of previous research [36]. We selected up-regulated metal transporters and constructed an ion exchange pattern diagram based on subcellular localization predictions (Figure 7B); we found that the expression of the K^+/H^+ antiporter (KEA) and $\text{Mg}^{2+}/\text{H}^+$ exchanger (MHX) was also up-regulated to mediate the response to salt stress, and these genes were co-expressed in the roots and leaves. This result suggests that the transport of Mg and K also contributes to stabilizing ion homeostasis in *M. niedzwetzkyana* under saline-alkali conditions; these findings enhance our understanding of the apple salt resistance mechanism.

TFs play a key role in plant abiotic stress responses, and WRKY TFs are highly involved in these processes. *MbWRKY5* and *MdWRKY30* enhance tolerance to drought and salt in tobacco and Arabidopsis, respectively, by regulating the expression levels of genes associated with stress responses; these genes are involved in alleviating oxidative stress and maintaining the integrity of the cell membrane [49,50]. *MdWRKY56* has previously been identified as a positive regulator of drought tolerance, and transgenic apple plants overexpressing the gene encoding this TF have a higher PRO content and antioxidant enzyme activities [51]. However, no key TFs responsive to salt-alkali stress have been reported. Our research revealed several saline-alkali stress-related TFs; a significant number of WRKY TFs that might play essential roles in regulating antioxidant enzyme activity and ion transport, such as *MdWRKY10*, *MdWRKY23*, and *MdWRKY31*, were identified. Notably, *MdWRKY31* is significantly up-regulated in the roots under saline-alkali stress. Furthermore, we characterized the expression of *MdCIPK29* and *MdPP2C29Like*, which encode protein kinases from the PP2C and CIPK families, in the leaves and roots, respectively, involved in the response to saline-alkali stress. We hypothesize that these key TFs might interact with protein kinases to regulate antioxidant enzyme activity and maintain ion homeostasis under saline-alkali stress. Additional studies are needed to clarify the functions of these TF genes in transgenic apple plants under saline-alkali stress. Additional studies are needed to experimentally verify interactions between TFs, protein kinases, and functional genes.

In summary, we have identified a potential regulatory strategy for enhancing saline-alkali stress tolerance in *M. niedzwetzkyana*. First, root cells were the first to sense saline-alkali stress, and second messengers such as ROS and Ca^{2+} transmitted external signals into the cytoplasm. Inside the cell, calcium-regulated pathways and phosphatases, such as

PP2C, are activated, altering the global transcriptional profile (inducing the expression of stress-associated transcription factors such as WKRY, MYB, and NAC) in *M. niedzwetzkyana*. Subsequently, genes encoding proteins related to salinity stress response were also induced to be expressed, including ion transport proteins and ROS scavenging proteins (e.g., *MdKEA5*, *MdMHX*, *MdPOD51*, *MdCAT1Like*). Ultimately, the resistance pathway is activated to maintain ion and reactive oxygen species homeostasis, promoting apple resistance and adaptation to saline-alkali stress.

5. Conclusions

The results of our study indicate that *M. niedzwetzkyana* is highly resistant to saline-alkali stress, and this is mediated by major morphological, physiological, and transcriptomic changes. Transcriptomic data showed that a large number of DEGs related to CAT, SOD, POD, and PPO were induced to express several candidate genes encoding various enzymes involved in saline-alkali resistance, including *MdPOD51*, *MdPOD57*, *MdCAT1Like*, and *MdPPO*, which were identified. The expression of some genes encoding transporters, protein kinases, and TFs, such as *MdMHX*, *MdKEA5*, *MdWRKY2*, *MdCIPK29*, and *MdPP2C29Like*, was up-regulated, suggesting that ion transport and molecular regulation systems are related to the saline-alkali tolerance of *M. niedzwetzkyana*. The results of our study indicate that the mechanism underlying the response of *M. niedzwetzkyana* to saline-alkali stress is complex. Our findings also revealed candidate genes involved in the response to saline-alkali stress and enhanced our understanding of the response of *M. niedzwetzkyana* to saline-alkali stress at the molecular level. Lastly, our findings will help breed improved apple varieties with enhanced saline-alkali resistance.

Supplementary Materials: The following supporting information can be downloaded at <https://www.mdpi.com/article/10.3390/horticulturae10050510/s1>, Figure S1: Correlation heat maps of t Pearson correlation for 18 samples. Table S1: Sample reads quality of 18 libraries. Table S2: Phenotypic data of 18 samples. Table S3: Primer sequences for RT-qPCR testing in this study.

Author Contributions: Conceived and designed the experiment: L.J. and Z.Z.; analyzed the data: L.J. and X.C.; wrote the manuscript: L.J. and Y.Y. All authors have read and agreed to the published version of the manuscript.

Funding: This research was funded by the Corps Key Areas of Science and Technology Research projects (no. 2021AB022), the Key Research and Development Programs of Shandong Province (no. 2021LZGC024; no. 2022LZGC010; no. 2022CXPT021), and the Natural Science Foundation of Shandong Province (no. ZR2020QC144).

Data Availability Statement: The supporting dataset is included in this study and the Supplementary Materials. The reads generated in this study were submitted to the Sequence Read Archive at the NCBI under accession number PRJNA1047940. The dataset can be accessed at the following URL: <http://www.ncbi.nlm.nih.gov/sra/> (accessed on 12 May 2024).

Acknowledgments: We would like to thank the anonymous reviewers for their valuable comments and helpful suggestions, which have helped to improve the manuscript.

Conflicts of Interest: The authors declare no conflict to interest.

References

1. Jesus, J.; Castro, F.; Niemelä, A.; Borges, M.T.; Danko, A.S. Evaluation of the Impact of Different Soil Salinization Processes on Organic and Mineral Soils. *Water Air Soil Pollut.* **2015**, *226*, 12. [CrossRef]
2. Nachshon, U. Cropland Soil Salinization and Associated Hydrology: Trends, Processes and Examples. *Water* **2018**, *10*, 1030. [CrossRef]
3. Li, J.G.; Pu, L.J.; Han, M.F.; Zhu, M.; Zhang, R.S.; Xiang, Y.Z. Soil salinization research in China: Advances and prospects. *J. Geogr. Sci.* **2014**, *24*, 943–960. [CrossRef]
4. Wang, N.; Zheng, Y.; Duan, N.; Zhang, Z.; Ji, X.; Jiang, S.; Sun, S.; Yang, L.; Bai, Y.; Fei, Z. Comparative transcriptomes analysis of red-and white-fleshed apples in an F1 population of *Malus sieversii* f. *niedzwetzkyana* crossed with *M. domestica* ‘Fuji’. *PLoS ONE* **2015**, *10*, e0133468. [CrossRef] [PubMed]

5. Duan, N.; Bai, Y.; Sun, H.; Wang, N.; Ma, Y.; Li, M.; Wang, X.; Jiao, C.; Legall, N.; Mao, L.; et al. Genome re-sequencing reveals the history of apple and supports a two-stage model for fruit enlargement. *Nat. Commun.* **2017**, *8*, 249. [[CrossRef](#)] [[PubMed](#)]
6. Lian, X.Y.; Zhao, X.Y.; Zhao, Q.; Wang, G.L.; Li, Y.Y.; Hao, Y.J. MdDREB2A in apple is involved in the regulation of multiple abiotic stress responses. *Hortic. Plant J.* **2021**, *7*, 197–208. [[CrossRef](#)]
7. Mei, C.; Yang, J.; Mei, Q.L.; Jia, D.F.; Yan, P.; Feng, B.B.; Mamat, A.; Gong, X.Q.; Guan, Q.M.; Mao, K.; et al. MdNAC104 positively regulates apple cold tolerance via CBF-dependent and CBF-independent pathways. *Plant Biotechnol. J.* **2023**, *21*, 2057–2073. [[CrossRef](#)] [[PubMed](#)]
8. Ren, Y.R.; Yang, Y.Y.; Zhao, Q.; Zhang, T.E.; Wang, C.K.; Hao, Y.J.; You, C.X. MdCIB1, an apple bHLH transcription factor, plays a positive regulator in response to drought stress. *Environ. Exp. Bot.* **2021**, *188*, 11. [[CrossRef](#)]
9. Li, J.; Yang, Y.Q. How do plants maintain pH and ion homeostasis under saline-alkali stress? *Front. Plant Sci.* **2023**, *14*, 1217193. [[CrossRef](#)]
10. Zhang, J.-T.; Mu, C.-S. Effects of saline and alkaline stresses on the germination, growth, photosynthesis, ionic balance and anti-oxidant system in an alkali-tolerant leguminous forage *Lathyrus quinquerivius*. *Soil Sci. Plant Nutr.* **2009**, *55*, 685–697. [[CrossRef](#)]
11. Guo, R.; Shi, L.X.; Yang, Y.F. Germination, growth, osmotic adjustment and ionic balance of wheat in response to saline and alkaline stresses. *Soil Sci. Plant Nutr.* **2009**, *55*, 667–679. [[CrossRef](#)]
12. Ondrasek, G.; Rathod, S.; Manohara, K.K.; Gireesh, C.; Anantha, M.S.; Sakhare, A.S.; Parmar, B.; Yadav, B.K.; Bandumula, N.; Raihan, F.; et al. Salt Stress in Plants and Mitigation Approaches. *Plants* **2022**, *11*, 717. [[CrossRef](#)] [[PubMed](#)]
13. Janku, M.; Luhová, L.; Petrivalsky, M. On the Origin and Fate of Reactive Oxygen Species in Plant Cell Compartments. *Antioxidants* **2019**, *8*, 105. [[CrossRef](#)] [[PubMed](#)]
14. Xu, Y.; Lu, J.H.; Zhang, J.D.; Liu, D.K.; Wang, Y.; Niu, Q.D.; Huang, D.D. Transcriptome revealed the molecular mechanism of *Glycyrrhiza inflata* root to maintain growth and development, absorb and distribute ions under salt stress. *BMC Plant Biol.* **2021**, *21*, 599. [[CrossRef](#)] [[PubMed](#)]
15. Chrysargyris, A.; Papakyriakou, E.; Petropoulos, S.A.; Tzortzakos, N. The combined and single effect of salinity and copper stress on growth and quality of *Mentha spicata* plants. *J. Hazard. Mater.* **2019**, *368*, 584–593. [[CrossRef](#)] [[PubMed](#)]
16. Ganapati, R.K.; Naveed, S.A.; Zafar, S.; Wang, W.; Xu, J. Saline-Alkali Tolerance in Rice: Physiological Response, Molecular Mechanism, and QTL Identification and Application to Breeding. *Rice Sci.* **2022**, *29*, 412–434. [[CrossRef](#)]
17. Martínez-Cuenca, M.-R.; Legaz, F.; Forner-Giner, M.Á.; Primo-Millo, E.; Iglesias, D.J. Bicarbonate blocks iron translocation from cotyledons inducing iron stress responses in Citrus roots. *J. Plant Physiol.* **2013**, *170*, 899–905. [[CrossRef](#)] [[PubMed](#)]
18. Ji, H.; Pardo, J.M.; Batelli, G.; Van Oosten, M.J.; Bressan, R.A.; Li, X. The Salt Overly Sensitive (SOS) Pathway: Established and Emerging Roles. *Mol. Plant* **2013**, *6*, 275–286. [[CrossRef](#)]
19. Lin, H.; Yang, Y.; Quan, R.; Mendoza, I.; Wu, Y.; Du, W.; Zhao, S.; Schumaker, K.S.; Pardo, J.M.; Guo, Y. Phosphorylation of SOS3-LIKE CALCIUM BINDING PROTEIN8 by SOS2 Protein Kinase Stabilizes Their Protein Complex and Regulates Salt Tolerance in Arabidopsis. *Plant Cell* **2009**, *21*, 1607–1619. [[CrossRef](#)]
20. Qiu, Q.-S.; Guo, Y.; Dietrich, M.A.; Schumaker, K.S.; Zhu, J.-K. Regulation of SOS1, a plasma membrane Na⁺/H⁺ exchanger in Arabidopsis thaliana, by SOS2 and SOS3. *Proc. Natl. Acad. Sci. USA* **2002**, *99*, 8436–8441. [[CrossRef](#)]
21. Shi, H.; Ishitani, M.; Kim, C.; Zhu, J.-K. The Arabidopsis thaliana salt tolerance gene SOS1 encodes a putative Na⁺/H⁺ antiporter. *Proc. Natl. Acad. Sci. USA* **2000**, *97*, 6896–6901. [[CrossRef](#)] [[PubMed](#)]
22. Wang, C.T.; Chen, Q.; Xiang, N.; Liu, Y.Y.; Kong, X.X.; Yang, Y.P.; Hu, X.Y. SIP1, a novel SOS2 interaction protein, is involved in salt-stress tolerance in Arabidopsis. *Plant Physiol. Biochem.* **2018**, *124*, 167–174. [[CrossRef](#)]
23. Wu, H.; Shabala, L.; Zhou, M.; Su, N.; Wu, Q.; Ul-Haq, T.; Zhu, J.; Mancuso, S.; Azzarello, E.; Shabala, S. Root vacuolar Na⁺ sequestration but not exclusion from uptake correlates with barley salt tolerance. *Plant J.* **2019**, *100*, 55–67. [[CrossRef](#)] [[PubMed](#)]
24. Xu, K.; Hong, P.; Luo, L.; Xia, T. Overexpression of AtNHX1, a Vacuolar Na⁺/H⁺ Antiporter from *Arabidopsis thaliana*, in *Petunia hybrida* Enhances Salt and Drought Tolerance. *J. Plant Biol.* **2009**, *52*, 453–461. [[CrossRef](#)]
25. Zhang, Y.M.; Zhang, H.M.; Liu, Z.H.; Li, H.C.; Guo, X.L.; Li, G.A. The wheat NHX antiporter gene TaNHX2 confers salt tolerance in transgenic alfalfa by increasing the retention capacity of intracellular potassium. *Plant Mol. Biol.* **2015**, *87*, 317–327. [[CrossRef](#)] [[PubMed](#)]
26. Mittler, R.; Vanderauwera, S.; Suzuki, N.; Miller, G.; Tognetti, V.B.; Vandepoele, K.; Gollery, M.; Shulaev, V.; Van Breusegem, F. ROS signaling: The new wave? *Trends Plant Sci.* **2011**, *16*, 300–309. [[CrossRef](#)]
27. Farooq, M.A.; Niazi, A.K.; Akhtar, J.; Saifullah; Farooq, M.; Souiri, Z.; Karimi, N.; Rengel, Z. Acquiring control: The evolution of ROS-Induced oxidative stress and redox signaling pathways in plant stress responses. *Plant Physiol. Biochem.* **2019**, *141*, 353–369. [[CrossRef](#)]
28. Pan, Y.; Wu, L.J.; Yu, Z.L. Effect of salt and drought stress on antioxidant enzymes activities and SOD isoenzymes of liquorice (*Glycyrrhiza uralensis* Fisch). *Plant Growth Regul.* **2006**, *49*, 157–165. [[CrossRef](#)]
29. Fini, A.; Guidi, L.; Ferrini, F.; Brunetti, C.; Di Ferdinando, M.; Biricolti, S.; Pollastri, S.; Calamai, L.; Tattini, M. Drought stress has contrasting effects on antioxidant enzymes activity and phenylpropanoid biosynthesis in *Fraxinus ornus* leaves: An excess light stress affair? *J. Plant Physiol.* **2012**, *169*, 929–939. [[CrossRef](#)]

30. Nakabayashi, R.; Yonekura-Sakakibara, K.; Urano, K.; Suzuki, M.; Yamada, Y.; Nishizawa, T.; Matsuda, F.; Kojima, M.; Sakakibara, H.; Shinozaki, K.; et al. Enhancement of oxidative and drought tolerance in Arabidopsis by overaccumulation of antioxidant flavonoids. *Plant J.* **2014**, *77*, 367–379. [[CrossRef](#)]
31. Dong, Q.L.; Liu, D.D.; An, X.H.; Hu, D.G.; Yao, Y.X.; Hao, Y.J. MdVHP1 encodes an apple vacuolar H(+)-PPase and enhances stress tolerance in transgenic apple callus and tomato. *J. Plant Physiol.* **2011**, *168*, 2124–2133. [[CrossRef](#)] [[PubMed](#)]
32. Chou, K.C.; Shen, H.B. Plant-mPLOC: A Top-Down Strategy to Augment the Power for Predicting Plant Protein Subcellular Localization. *PLoS ONE* **2010**, *5*, e11335. [[CrossRef](#)] [[PubMed](#)]
33. Cao, Y.B.; Song, H.F.; Zhang, L.Y. New Insight into Plant Saline-Alkali Tolerance Mechanisms and Application to Breeding. *Int. J. Mol. Sci.* **2022**, *23*, 16048. [[CrossRef](#)] [[PubMed](#)]
34. Forni, C.; Duca, D.; Glick, B.R. Mechanisms of plant response to salt and drought stress and their alteration by rhizobacteria. *Plant Soil* **2017**, *410*, 335–356. [[CrossRef](#)]
35. Yu, Z.P.; Duan, X.B.; Luo, L.; Dai, S.J.; Ding, Z.J.; Xia, G.M. How Plant Hormones Mediate Salt Stress Responses. *Trends Plant Sci.* **2020**, *25*, 1117–1130. [[CrossRef](#)]
36. Yang, J.; Li, W.; Guo, X.; Chen, P.; Cheng, Y.; Mao, K.; Ma, F. Cation/Ca²⁺ Exchanger 1 (MdCCX1), a Plasma Membrane-Localized Na⁺ Transporter, Enhances Plant Salt Tolerance by Inhibiting Excessive Accumulation of Na⁺ and Reactive Oxygen Species. *Front. Plant Sci.* **2021**, *12*, 746189. [[CrossRef](#)]
37. Yin, Y.-C.; Zhang, X.-D.; Gao, Z.-Q.; Hu, T.; Liu, Y. The Research Progress of Chalcone Isomerase (CHI) in Plants. *Mol. Biotechnol.* **2019**, *61*, 32–52. [[CrossRef](#)]
38. Jiang, W.; Yin, Q.; Wu, R.; Zheng, G.; Liu, J.; Dixon, R.A.; Pang, Y. Role of a chalcone isomerase-like protein in flavonoid biosynthesis in Arabidopsis thaliana. *J. Exp. Bot.* **2015**, *66*, 7165–7179. [[CrossRef](#)]
39. Deinlein, U.; Stephan, A.B.; Horie, T.; Luo, W.; Xu, G.H.; Schroeder, J.I. Plant salt-tolerance mechanisms. *Trends Plant Sci.* **2014**, *19*, 371–379. [[CrossRef](#)]
40. Zhang, M.J.; Liu, Y.L.; Han, G.L.; Zhang, Y.; Wang, B.S.; Chen, M. Salt tolerance mechanisms in trees: Research progress. *Trees* **2021**, *35*, 717–730. [[CrossRef](#)]
41. Zhang, J.; Sun, X.L. Recent advances in polyphenol oxidase-mediated plant stress responses. *Phytochemistry* **2021**, *181*, 112588. [[CrossRef](#)] [[PubMed](#)]
42. Liu, D.; Meng, S.; Xiang, Z.; Yang, G.; He, N. An R1R2R3 MYB Transcription Factor, MnMYB3R1, Regulates the Polyphenol Oxidase Gene in Mulberry (*Morus notabilis*). *Int. J. Mol. Sci.* **2019**, *20*, 2602. [[CrossRef](#)] [[PubMed](#)]
43. Plett, D.C.; Moller, I.S. Na plus transport in glycophytic plants: What we know and would like to know. *Plant Cell Environ.* **2010**, *33*, 612–626. [[CrossRef](#)]
44. Munns, R.; Gilliam, M. Salinity tolerance of crops-what is the cost? *New Phytol.* **2015**, *208*, 668–673. [[CrossRef](#)] [[PubMed](#)]
45. Wakeel, A.; Farooq, M.; Qadir, M.; Schubert, S. Potassium Substitution by Sodium in Plants. *Crit. Rev. Plant Sci.* **2011**, *30*, 401–413. [[CrossRef](#)]
46. Manaa, A.; Faurobert, M.; Valot, B.; Bouchet, J.-P.; Grasselly, D.; Causse, M.; Ahmed, H.B. Effect of Salinity and Calcium on Tomato Fruit Proteome. *OMICS J. Integr. Biol.* **2013**, *17*, 338–352. [[CrossRef](#)]
47. Sun, M.-H.; Ma, Q.-J.; Liu, X.; Zhu, X.-P.; Hu, D.-G.; Hao, Y.-J. Molecular cloning and functional characterization of MdNHX1 reveals its involvement in salt tolerance in apple calli and Arabidopsis. *Sci. Hort.* **2017**, *215*, 126–133. [[CrossRef](#)]
48. Sun, Z.; Li, J.; Guo, D.; Wang, T.; Tian, Y.; Ma, C.; Liu, X.; Wang, C.; Zheng, X. Melatonin enhances KCl salinity tolerance by maintaining K⁺ homeostasis in *Malus hupehensis*. *Plant Biotechnol. J.* **2023**, *21*, 2273–2290. [[CrossRef](#)] [[PubMed](#)]
49. Han, D.G.; Hou, Y.J.; Wang, Y.F.; Ni, B.X.; Li, Z.T.; Yang, G.H. Overexpression of a *Malus baccata* WRKY transcription factor gene (MbWRKY5) increases drought and salt tolerance in transgenic tobacco. *Can. J. Plant Sci.* **2019**, *99*, 173–183. [[CrossRef](#)]
50. Dong, Q.; Zheng, W.; Duan, D.; Huang, D.; Wang, Q.; Liu, C.; Li, C.; Gong, X.; Li, C.; Mao, K.; et al. MdWRKY30, a group IIa WRKY gene from apple, confers tolerance to salinity and osmotic stresses in transgenic apple callus and Arabidopsis seedlings. *Plant Sci.* **2020**, *299*, 110611. [[CrossRef](#)]
51. Duan, D.; Yi, R.; Ma, Y.; Dong, Q.; Mao, K.; Ma, F. Apple WRKY transcription factor MdWRKY56 positively modulates drought stress tolerance. *Environ. Exp. Bot.* **2023**, *212*, 105400. [[CrossRef](#)]

Disclaimer/Publisher’s Note: The statements, opinions and data contained in all publications are solely those of the individual author(s) and contributor(s) and not of MDPI and/or the editor(s). MDPI and/or the editor(s) disclaim responsibility for any injury to people or property resulting from any ideas, methods, instructions or products referred to in the content.